SLAC–PUB–8229
September 1999

Optimization of NLC machine parameters for specific physics processes*

K.A. Thompson, T.O. Raubenheimer, T.L. Barklow
Stanford Linear Accelerator Center, Stanford University, Stanford, CA 94309

Abstract

We examine the optimization of NLC parameters at 500, 1000, and 1500 GeV c.m. energy for specific classes of physics processes, in particular, top and stop pair production, and W-W scattering processes. Our focus is on optimizing the luminosity spectrum, while maintaining or improving machine operability.

Presented at Worldwide Study on Physics and Experiments with Future Linear e+e- Colliders, April 28 - May 5, 1999, Sitges (Barcelona), Spain

*Work supported by Department of Energy contract DE–AC03–76SF00515.

Optimization of NLC machine parameters for specific physics processes

K.A. Thompson, T.O. Raubenheimer, T.L. Barklow
Stanford Linear Accelerator Center, P.O.Box 4349, Mail Stop 26, Stanford, CA 94309, USA

We examine the optimization of NLC parameters at 500, 1000, and 1500 GeV c.m. energy for specific classes of physics processes, in particular, top and stop pair production, and W-W scattering processes. Our focus is on optimizing the luminosity spectrum, while maintaining or improving machine operability.

1 Introduction

The purpose of this paper is to look at the flexibility in optimizing the event rate for specific classes of physics processes in a future linear collider. We do not address the issue of detector backgrounds, other than to observe that increasing n_γ (number of beamstrahlung photons per incoming particle) and Υ (the beamstrahlung parameter, which governs the rate of coherent pair production) much higher than the values in the present designs would substantially increase backgrounds in the detector. With this caveat, our working assumption is that when the total rate for the various processes considered is optimized, one will end up with a larger number of useful events even after appropriate cuts are applied to reduce backgrounds.

Table 1: IP parameters for three ~1/2 TeV c.m. and three ~1 TeV c.m. NLC designs[2]

	A-500	B-500	C-500	A-1000	B-1000	C-1000
E_{beam} [GeV]	267.5	257.5	250.	523.	504.	489.
N [10^{10}]	0.75	0.95	1.1	0.75	0.95	1.1
$\gamma\epsilon_x/\gamma\epsilon_y$ [μm-r]	4./0.06	4.5/0.1	5./0.14	4./0.06	4.5/0.1	5./0.14
β_x/β_y [mm]	10/0.1	12/0.12	13/0.2	10/0.125	12/0.15	13/0.2
σ_z [μm]	90.	120.	145.	90.	120.	145.
σ_x/σ_y [nm]	276/3.4	327/4.9	365/7.6	198/2.7	234/3.9	261/5.4
Υ_{avg}	0.14	0.11	0.09	0.39	0.30	0.25
H_D	1.36	1.30	1.49	1.50	1.44	1.50
n_γ	1.08	1.18	1.24	1.39	1.53	1.62
δ_B	4.3%	3.9%	3.7%	9.5%	9.2%	8.7%
Bunches/train	95	95	95	95	95	95
Rep. rate	120	120	120	120	120	120
$L_D/10^{33}/\mathrm{cm}^2/\mathrm{sec}$	7.42	6.66	5.94	14.33	12.95	11.67

We focus on processes whose cross sections are increasing over the energy ranges of interest; optimization for a sharp luminosity spectrum at the top threshold is addressed elsewhere at this conference[1]. One factor in maximizing the event rate is obviously to maximize the convolution of the cross section with the beamstrahlung-degraded luminosity spectrum. However, the difficulty of machine operation is an important factor in determining the event rates one will actually obtain. The

vertical spot size is very small in the nominal linear collider designs, which leads to tight vertical machine tolerances. Thus it is also of interest to see how one can relax these tolerances with minimal impact on the luminosity.

We present some interaction region parameters[2] for the basic NLC designs near 0.5, 1.0, and 1.5 TeV c.m. energy in Tables 1 and 2. The luminosities, the number of photons n_γ, and the average fractional beamstrahlung energy loss δ_B are obtained from simulations using the beam-beam code Guineapig[3].

Note that the c.m. energy is assumed to decrease with higher bunch charge N because the beam loading reduces the acceleration gradient in a given linac design; it is possible to compensate the loading by adding additional rf structures, but this increases the cost. There is also variation in other parameters among different design versions near a given energy. We have done systematic studies[4] where we vary each of the parameters N, σ_z, β_x, β_y, $\gamma\epsilon_y$, or $\gamma\epsilon_x$. We find that the best "knobs" for increasing luminosity at the high energy end of the spectrum are $\gamma\epsilon_y$ and N. It is thought difficult to decrease $\gamma\epsilon_y$ much, but one may consider increasing N if one is willing either to let the energy drop or compensate for the beam-loading.

One finding of these studies is that doubling β_y (which relaxes vertical tolerances) does not reduce luminosity very much[4]. We have also examined designs[5] with equal or near-equal beta functions (see Table 4) which increase the vertical spot size even further and can have much higher total luminosity if one is willing to allow rather high values of n_γ and Υ. To bring n_γ and Υ down to more conventional values, we can reduce the bunch charge, sacrificing some of the luminosity gain. Note that in the last two designs in Table 4, we assume the bunch spacing is halved, the number of bunches doubled, and the charge per bunch decreased. The design with bunch charge $N = 0.475 \times 10^{10}$ has the same beam loading as the nominal NLC-B-1000 design. The total luminosity of this design is comparable to the nominal NLC-B-1000 design but the spectrum is somewhat more degraded to lower energies (δ_B=16% instead of 9%). The design with $N = 0.55 \times 10^{10}$ has higher luminosity, but it would be necessary to make up for increased beam loading if one wanted to keep the nominal c.m. energy the same.

We show the luminosity spectra for the nominal designs, with effects of both beamstrahlung and initial state radiation (ISR) included, in Table 3. The fractional luminosities are shown, e.g., $L_{99\%}$ denotes the percentage of the luminosity with c.m. energy greater than or equal to 99% of the nominal c.m. energy. (These numbers are not significantly different for the A, B, and C variations of the designs at 500 and 1000 GeV.)

2 SUSY scalar production

We compare the rates of top and stop production in a 500-GeV collider, assuming $m_{\tilde{t}} = m_t$. The total top and stop pair production cross-sections are plotted in Figure 1.

The production rates (# events in a running year of 10^7 sec) are shown in Table 5 for the three nominal designs near 500-GeV c.m. energy, and also for designs with bunch charge N pushed up from the nominal B-500 design value. Here we

Table 2: IP parameters for two ∼1.5 TeV c.m. NLC designs

	A-1500	B-1500
E_{beam} [GeV]	703	739
N [10^{10}]	1.4	0.95
$\gamma\epsilon_x/\gamma\epsilon_y$ [μm-r]	4.5/0.14	4.5/0.1
β_x/β_y [mm]	15/0.2	13/0.2
σ_z [μm]	130.	150.
σ_x/σ_y [nm]	222/4.5	201/3.7
Υ_{avg}	0.60	0.41
H_D	1.61	1.50
n_γ	2.2	1.7
δ_B	17%	12%
Bunches/train	95	95
Rep. rate	60	90
$L_D/10^{33}/\mathrm{cm}^2/\mathrm{sec}$	14.3	12.3

Table 3: Fractional luminosities for NLC designs

	∼500 GeV designs	∼1000 GeV designs	1500-A	1500-B
beamst.+ISR:				
$L_{99.5\%}$ (sim)	37%	27%	18%	23%
$L_{99\%}$ (sim)	44%	33%	22%	29%
$L_{98\%}$ (sim)	54%	41%	28%	36%
$L_{95\%}$ (sim)	69%	56%	41%	50%
$L_{90\%}$ (sim)	81%	70%	55%	64%
$L_{80\%}$ (sim)	91%	84%	73%	80%
$L_{50\%}$ (sim)	98%	97%	95%	97%

assume it is reasonable to compensate the extra beam loading to keep the energy fixed.

3 WW-scattering processes

The class of processes $e^+e^- \to \ell\ell X$ occurring via WW scattering, where one or both ℓ's is a neutrino and X could be for example $t\bar{t}$, W's and/or Z's, have cross sections which rise with energy above threshold and through the TeV energy scale. Taking as a representative example the process $e^+e- \to \nu_e\bar{\nu}_e W^+W^-$, we show the number of events in 10^7 seconds of running for designs near 1 TeV in Table 6. In addition to the nominal A, B, and C designs, we show the increase in luminosity attainable with $\gamma\epsilon_y$ decreased from its nominal value of 0.1μm-r, or with N increased from its nominal value of 0.95×10^{10}, with and without compensation of the extra beam-loading. The biggest luminosity gains are obtained by increasing N and keeping the energy fixed, or by going to equal or near-equal beta functions and keeping N near its nominal

Table 4: IP parameters for ∼1.0 TeV c.m. NLC designs, with equal or near-equal beta functions

	A-1000-bx1by1	B-1000-bx1.3by1.3	A-1000-bx2.5by1	B-1000-bx1.3by1.3 N.475-b190	B-1000-bx1.3by1.3 N.55-b190
E_{beam} [GeV]	523	504	523	504	504
N [10^{10}]	0.75	0.95	0.75	0.475	0.55
$\gamma\epsilon_x/\gamma\epsilon_y$ [μm-r]	4.0/0.06	4.5/0.1	4.0/0.06	4.5/0.1	4.5/0.1
β_x/β_y [mm]	1.0/1.0	1.3/1.3	2.5/1.0	1.3/1.3	1.3/1.3
σ_z [μm]	90.	120.	90.	120.	120.
σ_x/σ_y [nm]	62.5/7.7	77/11.5	99/7.7	77/11.5	77/11.5
$\mathcal{L}_0$ [10^{33} m^{-2}]	9.36	8.11	5.92	2.03	2.72
Υ_{eff}	1.9	1.5	0.83	0.50	0.62
$\mathcal{L}_D$ [10^{33} m^{-2}]	35.1	31.3	13.7	4.68	6.81
H_D	3.7	3.9	2.3	2.3	2.5
n_γ	4.7	5.1	2.6	2.2	2.7
δ_B	41%	40%	22%	16%	20%
Bunches/train	95	95	95	190	190
Rep. rate	120	120	120	120	120
$L_D/10^{33}$/cm^2/sec	40.0	35.7	15.6	10.7	15.5

value; further study is needed to see how high n_γ and Υ can be allowed to go. Note that there is only a 13% reduction in the number of events for the case where β_y is doubled from its nominal value. Also, note that we can get event rates comparable to those for the nominal designs in the equal-beta, reduced charge-per-bunch designs B-1000-bx1.3by1.3-N.475-b190 and B-1000-bx1.3by1.3-N.55-b190, which have greatly relaxed vertical tolerances. Similar trends hold for the designs near 1.5 TeV; some examples are shown in Table 7.

Table 5: Number of top and stop pair production events in a 10^7 second running year, for nominal designs near 1/2 TeV c.m. (first three columns) and for modified B-500 design with increased N and energy kept fixed (last three columns).

	A-500	B-500	C-500	B-N1.1	B-N1.3	B-N1.5
$e^-_L e^+_R \to t\bar{t}$	785000	674000	581000	927000	1347000	1856000
$e^-_R e^+_L \to t\bar{t}$	357000	305000	262000	420000	609000	837700
$e^-_L e^+_R \to \tilde{t}_R\bar{\tilde{t}}_R$	22000	17500	14200	23900	34000	46000
$e^-_R e^+_L \to \tilde{t}_R\bar{\tilde{t}}_R$	92000	74000	60200	101000	144000	195000
$e^-_L e^+_R \to \tilde{t}_L\bar{\tilde{t}}_L$	178000	143000	116500	195000	279000	377000
$e^-_R e^+_L \to \tilde{t}_L\bar{\tilde{t}}_L$	4900	3900	3200	5300	7600	10200

Table 6: Rate of events for designs near 1 TeV c.m., for the process $e^+e^- \to \nu\bar{\nu}W^+W^-$ (assuming $M_H = 100$ GeV and no polarization)

	No. of events	% change B-1000	n_γ
A-1000	76000	+28%	1.4
B-1000	59300	0%	1.5
C-1000	48300	-19%	1.6
B-1000, $\gamma\epsilon_y \downarrow 0.08\mu$m-r	68200	+15%	1.5
B-1000, $\gamma\epsilon_y \downarrow 0.06\mu$m-r	80300	+35%	1.5
B-1000, $\gamma\epsilon_y \downarrow 0.04\mu$m-r	102000	+73%	1.5
B-1000, N $\uparrow 1.1{\cdot}10^{10}$	81170	+37%	1.8
B-1000, N $\uparrow 1.3{\cdot}10^{10}$	114000	+92%	2.0
B-1000, N $\uparrow 1.5{\cdot}10^{10}$	152000	+157%	2.3
B-1000, N $\uparrow 1.1{\cdot}10^{10}$, E$\downarrow$978 GeV	72400	+22%	1.8
B-1000, N $\uparrow 1.3{\cdot}10^{10}$, E$\downarrow$935 GeV	84300	+42%	2.0
B-1000, N $\uparrow 1.5{\cdot}10^{10}$, E$\downarrow$891 GeV	92600	+56%	2.3
A-1000-bx1by1	123000	+107%	4.7
B-1000-bx1.3by1.3	95900	+62%	5.1
A-1000-bx2.5by1	70700	+19%	2.6
B-1000, $\beta_y \uparrow 0.30$ mm	51700	-13%	1.5
B-1000-bx1.3by1.3-N.475-b190	44900	-24%	2.2
B-1000-bx1.3by1.3-N.55-b190	61700	+4%	2.7
B-1000, $\beta_y \uparrow 0.30$ mm, N $\uparrow 1.5{\cdot}10^{10}$	130400	+120%	2.3
B-1000, $\beta_y \uparrow 0.30$ mm, N $\uparrow 1.5{\cdot}10^{10}$, E$\downarrow$891 GeV	71700	+21%	2.2

Table 7: Rate of events for designs near 1.5 TeV c.m., for the process $e^+e^- \to \nu\bar{\nu}W^+W^-$ (assuming $M_H = 100$ GeV and no polarization)

	No. of events	% change B-1500	% change B-1000	n_γ
A-1500	230000	-10%	290%	2.2
B-1500	254000	0%	330%	1.7
B-1500, N $\uparrow 1.1{\cdot}10^{10}$	345000	+36%	480%	2.0
B-1500, N $\uparrow 1.3{\cdot}10^{10}$	483000	+90%	710%	2.3
B-1500, N $\uparrow 1.5{\cdot}10^{10}$	646000	+154%	990%	2.6
B-1500, $\beta_y \uparrow 0.30$ mm	235000	-8%	300%	1.7

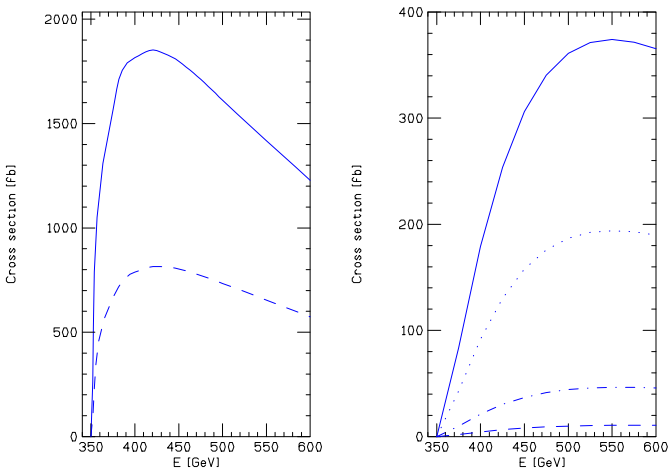

Figure 1: Left-hand plot shows cross sections for $e_L^- e_R^+ \to t\bar{t}$ (solid curve) and $e_R^- e_L^+ \to t\bar{t}$ (dashed curve). Right-hand plot shows cross sections for $e_L^- e_R^+ \to \tilde{t}_R \bar{\tilde{t}}_R$ (dot-dashed curve), $e_R^- e_L^+ \to \tilde{t}_R \bar{\tilde{t}}_R$ (dotted curve), $e_L^- e_R^+ \to \tilde{t}_L \bar{\tilde{t}}_L$ (solid curve), $e_R^- e_L^+ \to \tilde{t}_L \bar{\tilde{t}}_L$ (dashed curve).

Conclusions and Acknowledgments

The examples in this paper, representative of processes whose cross sections increase with energy, illustrate several approaches to increasing event rates beyond those which would be obtained in the nominal designs. The nominal designs appear to be fairly well optimized, although a significant increase in the vertical beta function (accompanied perhaps by some decrease in the horizontal beta function) may be desirable to relax the vertical tolerances in the collider, while maintaining luminosity at levels comparable to the nominal designs. The cases where there is a large (factor two or more) increase in event rate are accompanied by large n_γ and Υ and thus significantly higher backgrounds; just how much background is acceptable must be examined in more detail for individual physics channels.

We thank M.Peskin and L.Dixon for useful discussions and comments.

References

1. D.Cinabro, et.al., "Machine parameters and ttbar threshold study", this conference.
2. See http://www-project.slac.stanford.edu/lc/nlc-tech.html under Accelerator Physics parameters.
3. D.Schulte, Ph.D. thesis, 1996.
4. K.Thompson and T.Raubenheimer, NLC collider note LCC-0014 (1999).
5. K.Thompson and T.Raubenheimer, NLC collider note LCC-0022 (1999).